laminar compressible boundary layers," Separated Flows Research Project, Graduate Aeronautical Labs California Institute of Technology TR 2 (June 1, 1962)

[8] Denison, M R and Baum, E, "Compressible free shear layer with finite initial thickness," AIAA J 1, 342–349 (1963)

[9] Chapman, D R, "Laminar mixing of a compressible fluid," NACA Rept 958 (1950)

[10] Dewey, C F, Jr, 'Measurements in highly dissipative regions of hypersonic flows Part II The near wake of a blunt body at hypersonic speeds," Ph D Thesis, California Institute of Technology (1963)

[11] Chapman, D R, Kuehn, D M, and Larson H K, "Investigation of separated flows in supersonic and subsonic streams with emphasis on the effect of transition," NACA Rept 1356 (1958); this report supersedes NACA TM A55L14 (1956) and NACA TM 3869 (1957)

APRIL 1964 AIAA JOURNAL VOL 2, NO 4

A Study of Wakes behind a Circular Cylinder at $M = 5.7$

JOHN F McCARTHY JR *
North American Aviation, Inc, Downey, Calif

AND

TOSHI KUBOTA†
California Institute of Technology, Pasadena, Calif

The flow field behind a circular cylinder was investigated experimentally at a nominal Mach number of 5 7, over a range of Reynolds numbers from 4500 to 66,500, based on the cylinder diameter Pitot pressure, static pressure, and total temperature were measured at various distances behind three cylinders of different diameters in order to determine the flow properties in the wake The data at different Reynolds numbers were correlated in a manner indicated by a linearized theory for the laminar far wake with axial pressure gradient Transition from laminar to turbulent flow was determined from the velocity profiles and correlated with results obtained from mass-diffusion and hot-wire fluctuation measurements

Nomenclature

d = cylinder diameter
h = static enthalpy
M = Mach number
p = static pressure
p_0 = freestream stagnation pressure, absolute
p_{0g} = freestream stagnation pressure, gage
p_p = pitot pressure
Re_d = freestream Reynolds number based on cylinder diameter
Re_x = Reynolds number based on distance along wake and conditions at edge of boundary layer
Re_T = Townsend Reynolds number
T_{aw} = adiabatic wire temperature
u = component of velocity parallel to wake centerline
v = component of velocity normal to wake centerline
w = velocity defect, $1 - (u/u_e)$
x = length along wake centerline measured from center of cylinder
y = length normal to wake centerline measured from line through center of cylinder
ϵ_T = turbulent diffusivity
ω = angle of cylinder measured from stagnation point

Subscripts

e = conditions at outer edge of wake
m = measured
0 = initial conditions (usually taken at wake neck)

Introduction

THE nature of wakes is one of the oldest basic problems in the field of classical fluid mechanics Although the wakes in low-speed flow have been discussed in several treatises,[1–6] it was only recently that research was directed toward the phenomenon of high-speed flow The development of intercontinental ballistic missiles and hypersonic entry vehicles has kindled this interest in high-speed wakes

The theoretical problem of hypersonic wakes was first treated by Feldman,[7] who devised a simple model of the wake flow Feldman's basic approach has been extended by Lykoudis[8] More recently, Lees and Hromas[9] have attacked the problem of turbulent diffusion in the wake by using integral methods to solve the boundary-layer equations The two-dimensional laminar hypersonic wake with streamwise pressure gradient has been solved by Kubota,[10] using linearized equations

Perhaps the major obstacle in correlating theory and experiment in hypersonic wakes is the difficulty of obtaining reliable and detailed experimental data Atmospheric entry involves a range of temperature and Mach number that cannot be simulated effectively by known devices for extended periods Therefore, only limited data have been secured, either from short-duration experimental facilities, such as ballistic ranges[11] and shock tunnels[12] or from actual flight where results are not easily duplicated The conventional wind tunnel does not simulate the high Mach

Received June 6, 1963; revision received January 28, 1964 The work discussed in this paper was carried out under the sponsorship and with the financial support of the U S Army Research Office and the Advanced Research Projects Agency, Contract No DA-04-495-ORD-3231 This research is a part of Project DEFENDER sponsored by the Advanced Research Projects Agency This work also was supplemented by the Space and Information Systems Division of North American Aviation, Inc

* Director, Apollo Control Systems, Space and Information Systems Division Associate Fellow Member AIAA

† Associate Professor of Aeronautics Member AIAA

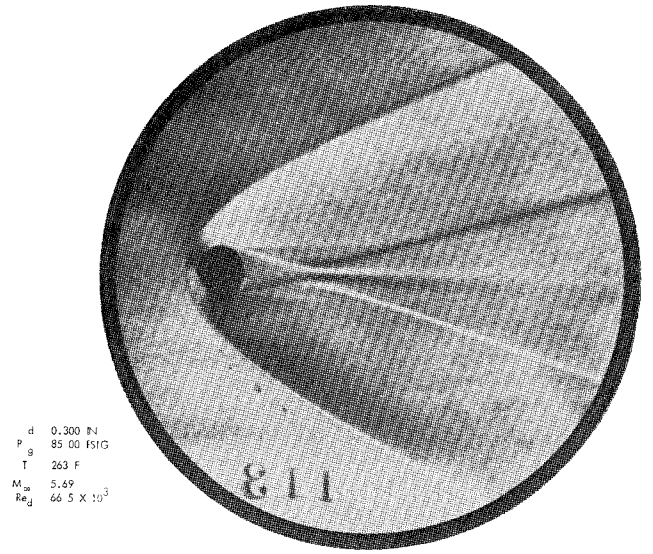

Fig 1 Schlieren photograph of the flow around cylinder

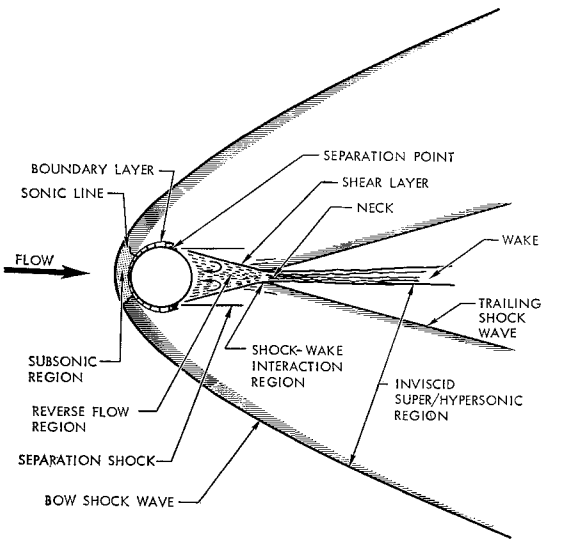

Fig 2 Local flow regimes

number and the high temperature attained during entry, but it does provide a means of measuring state properties throughout a hypersonic flow field One major advantage inherent in wind-tunnel testing is the capability of varying the Reynolds number independently of other quantities, enabling the Reynolds number effect to be determined explicitly A systematic hypersonic wake study program, employing the hypersonic wind tunnel as the experimental tool, has been in progress at Graduate Aeronautical Laboratory, California Institute of Technology (GALCIT) for some time For example, Demetriades[13] has investigated transition by hot-wire anemometry; Mohlenhoff[14] and Kingsland[15] have studied mixing by means of helium and argon diffusion; Dewey[16] investigated the base-flow region; and Behrens,[17] investigating the far wake by using thin, heated cylinders as models, is engaged in determining flow properties by means of hot-wire anemometry

The purpose of the present investigation was to determine experimentally the two-dimensional wake flow field behind a circular cylinder, as shown in Figs 1 and 2 Three state properties were selected for measurements: pitot pressure, static pressure, and total temperature

Experimental Techniques‡

GALCIT Hypersonic Wind Tunnel

All tests were conducted in the GALCIT hypersonic wind tunnel, leg 1, shown schematically in Fig 3 The test section of this tunnel is 5 in in width and $5\frac{1}{4}$ in in height The wind tunnel is a continuous-flow, closed-return device, with a nominal fixed Mach number of 5 7 at a distance of 17 34 in from the throat, where the model was ultimately placed, spanning the test section A complete description of the compressor and the associated instrumentation is given by Baloga and Nagamatsu [20]

The reservoir pressure was regulated between 0 00 and 100 00 psig, with an accuracy of ±0 02 psig and with corresponding Reynolds numbers between 33,000 and 260,000/in , based on freestream conditions The automatically controlled reservoir temperature can be varied between 225° and 325°F A reservoir temperature of 262°F, with accuracy of ±2°F, was selected for all tests This temperature closely approached the minimum without condensation effects for the nominal operating dew points

Table 1 summarizes the test conditions of the experiment The 3-to-1-ratio in model size and the 8-to-1 ratio in absolute stagnation pressure provided sufficient variation in Reynolds number to determine its effect on wake properties

Table 1 Test summary

Model d, in	p_{0g} psig	T_0, °F	$Re_d \times 10^{-3}$
0 300	85 00	263	66 5
0 300	60 00	263	49 4
0 300	35 00	262	32 7
0 300	10 00	262	16 7
0 200	96 68	264	49 3
0 200	59 48	263	32 7
0 200	22 48	262	16 6
0 200	3 80	260	8 58
0 100	59 42	263	16 3
0 100	22 54	262	8 28
0 100	3 84	260	4 29

‡ For detailed description of the experimental techniques, see Refs 18 and 19

Pitot-Pressure Measurements

The pitot pressure was measured by means of a small glass-tipped probe connected to a miniature wafer-type variable-reluctance pressure transducer This measurement (and subsequent ones) was displayed as vertical distance on an Autograph recorder

The pitot-pressure probe was moved axially and vertically from outside the tunnel by motor-driven lead screws Ori-

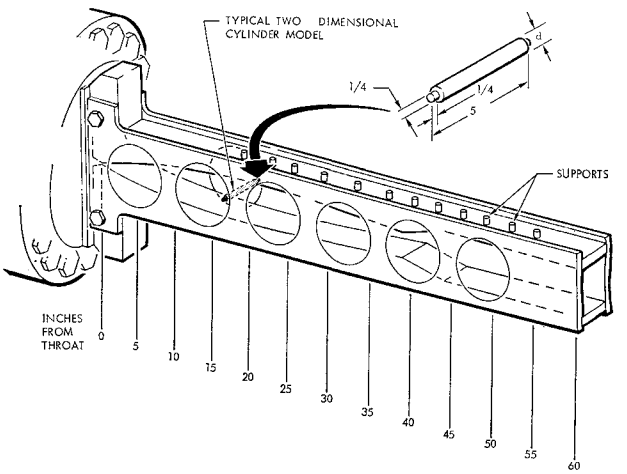

Fig 3 Model installations

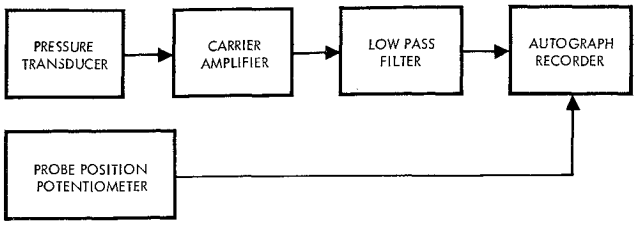

Fig 4 Pressure recording system

fice location was displayed as horizontal distance on the recorder by a rotary potentiometer on the gearing for positioning the probe The system block diagram is shown in Fig 4

Because flow inclinations up to 15° were encountered, measurements were made to determine the angle-of-attack sensitivity of the pitot probe The results of this calibration showed that the pitot probe is relatively insensitive to angle of attack in the range of interest Estimated accuracy of the pitot-pressure measurements is $\Delta p_p/p_0 = \pm 10^{-4}$

Pitot-pressure distributions at various stations are shown for two typical cases in Figs 5 and 6 Figure 5 represents a turbulent case, and Fig 6 represents a laminar case

Static-Pressure Measurements

The static pressure was measured by means of a small probe connected to a sensitive, variable-reluctance transducer located outside the wind tunnel

Several vertical static-pressure surveys were made at different axial locations for the various cylinders The static pressure was found to be constant across the wake and almost constant up to the trailing shock

To test the two-dimensionality of the flow field behind the cylindrical rod, the static-pressure distribution was measured in the horizontal direction parallel to the cylinder axis Surveys were made at various axial positions downstream of the 0 300- and 0 100-in models These surveys revealed that a disturbance originated ahead of the intersection of the model with the sidewalls of the wind tunnel As a result of these tests, the limits of two-dimensional flow were identified

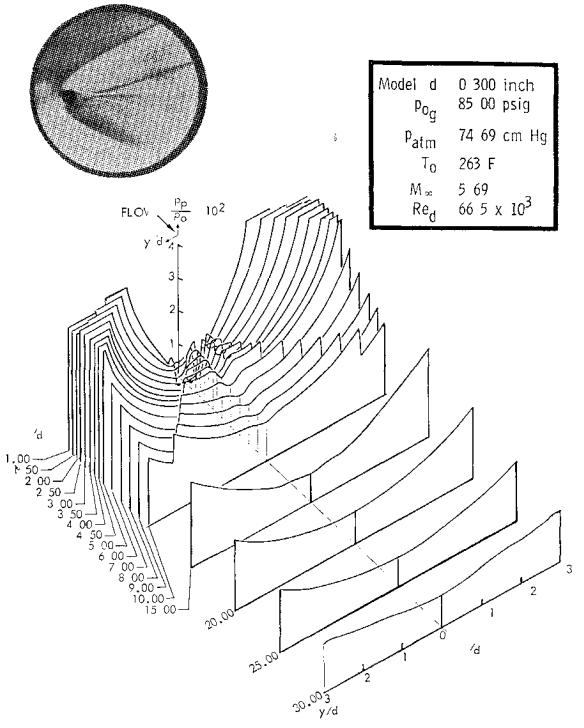

Fig 5 Pilot pressure, turbulent wake

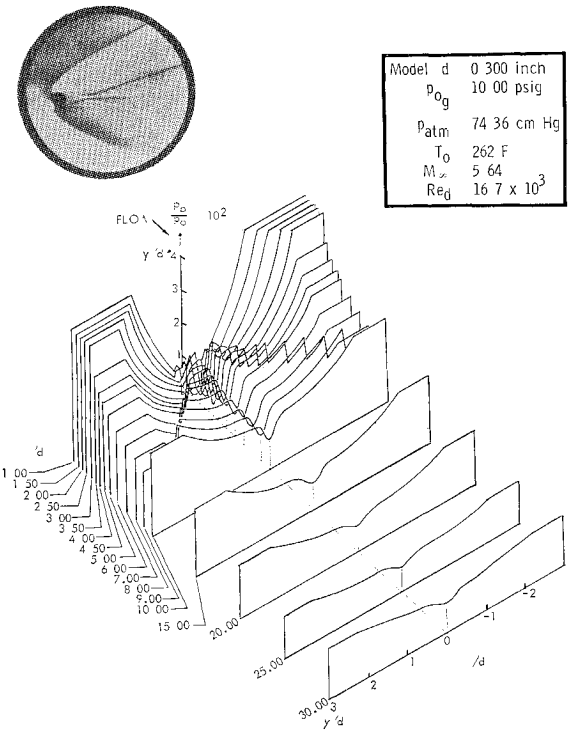

Fig 6 Pitot pressure, laminar wake

After establishing the variation of static pressure across the wake and identifying the boundaries of the two-dimensional flow region behind the model, static-pressure traces were taken along the centerline of the wind tunnel and behind the models for the 11 conditions cited in Table 1 The results of these tests are shown in Fig 7 Estimated accuracy of the static-pressure measurements is $\Delta p/p_\infty = \pm 0.005$

Since the orifices of the static-pressure probe were located a fixed distance behind the apex of the probe cone, it was not possible to measure static pressure close to the neck Consequently, it was necessary to estimate the static pressure in the vicinity of the neck from available data Because the axial gradient in static pressure is high in this region, a precise extrapolation upstream of the measured data is difficult unless the static pressure is known The static pressure slightly behind the neck was estimated by considering the base-flow region [18]

Base-Pressure Measurements

To extrapolate the measured static-pressure traces in the wake upstream, it was necessary to measure the base pressure of the model accurately Only the 0 300-in model was used because of the relatively large size of the static-pressure orifices on the smaller models A 0 009-in orifice represented the smallest practical diameter, corresponding to about 3° on the surface of the 0 300-in model

The cylinder was rotated to obtain the pressure distribution around it The distribution in the base region is shown in Fig 8 This figure also shows the data of Tewfik and Giedt,[21] whose experiments were made at a lower Reynolds number than the present tests In this figure, the region of reverse flow is evident, especially at high stagnation pressure Accuracy of the base-pressure measurements was estimated at $\Delta p(\omega)/p(0) = \pm 0.001$ for the test conditions at the higher stagnation pressures and ± 0.002 for those at the lower stagnation pressures

Total-Temperature Measurements

Total temperature was measured by an unshielded thermocouple with heated supports Heating of the supports was

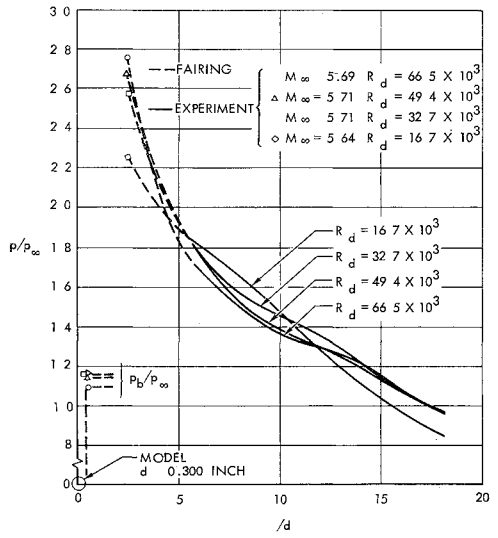

Fig 7a Axial static-pressure traces, 0 300-in -diam cylinder

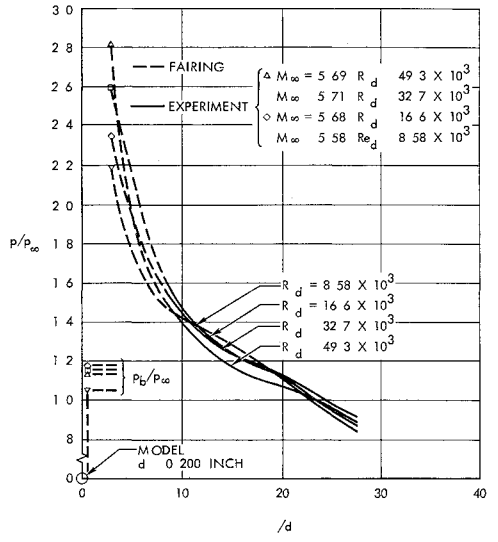

Fig 7b Axial static-pressure traces, 0 200-in -diam cylinder

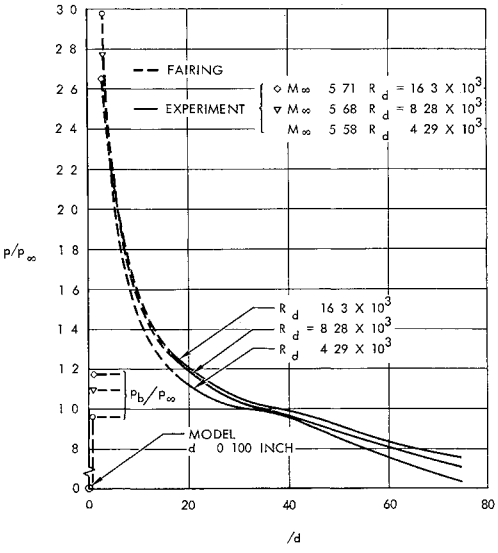

Fig 7c Axial static-pressure, traces 0 100-in -diam cylinder

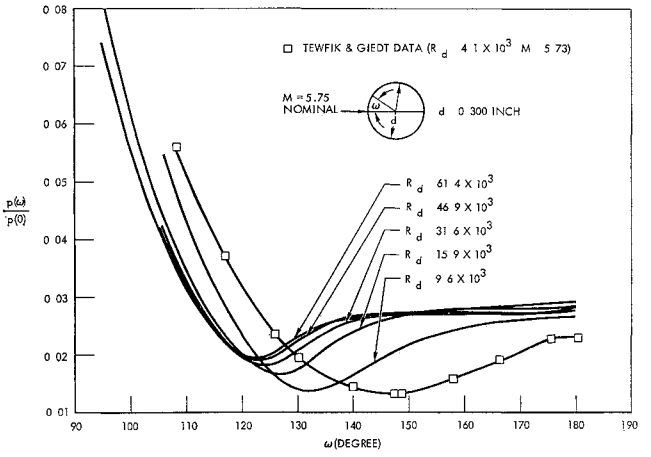

Fig 8 Experimental pressure distribution on cylinder

controlled, so that the support temperature was equal to the temperature indicated by the thermocouple

Because each total temperature trace required several hours, only surveys with the 0 300-in model were taken These traces were considered adequate for defining total-temperature variation in the wake as a function of Reynolds number, especially since the percentage variation of absolute temperature was small (except in the vicinity of the neck), even for laminar flow The accuracy of the theromocouple measurements is estimated at $\pm\frac{1}{2}$°F

Data Reduction

Reynolds number corrections to measured pitot pressures may be necessary for very low Reynolds numbers, but for the present tests, the outside diameter of the glass tip used for pitot measurements was chosen to preclude corrections when reducing the experimental data No account was taken of the effective displacement of streamlines caused by velocity gradients present in the wake This correction was estimated to be less than 10% of the wake width for the worst case, i e , in the vicinity of the neck

To correct the values of static pressure for boundary-layer effects, Mathews' data, which were taken for static-pressure probes of the same geometry as that used for the present tests, were used [22] A linear variation was assumed for the value of measured pressure to actual pressure, as a function of the viscous interaction parameter χ:

$$p_m/p = 1 + 0\,235\chi \qquad (1)$$

This variation is less than that for an insulated flat plate as discussed by Hayes and Probstein [23]

The temperature measured by the heated thermocouple is the adiabatic wire temperature associated with infinite aspect ratio The true total temperature was obtained from the measured adiabatic wire temperature by applying the correction for recovery factor This correction was accomplished with data based on Dewey's work For free-molecule flow and continuum flow, the ratios of adiabatic wire temperature to total temperatures are $\frac{7}{6}$ and 0 95, respectively

As noted in the preceding portions of this section, the accuracy of each measurement was carefully identified However, because of the many involved calculations necessary in obtaining final data, the accuracy of the final product can only be roughly estimated It is estimated that the over-all accuracy of the final experimental data is from 2 to 4% for the distributions of normalized velocity, static enthalpy, and total enthalpy (which will be described in the following section), except in the immediate region of the neck It is estimated that the computed absolute values of the centerline quantities are accurate to within 5% The major source of

error was the extrapolation of static pressure into the neck region

Results and Discussion

Using a linearized theory of laminar wake with streamwise pressure gradient, the following results were obtained [10, 18] Using the transformations

$$\bar{x}(x) = \int_0^x \frac{\rho_e \mu_e u_e}{\rho_\infty \mu_\infty u_\infty} \frac{dx}{d} \tag{2}$$

$$\bar{y}(x,y) = \frac{u}{u_\infty} (Re_d)^{1/2} \int_0^y \frac{\rho}{\rho_\infty} \frac{dy}{d} \tag{3}$$

then

$$M^2 w = \frac{A}{\bar{x}^{1/2}} \exp\left(-\frac{\bar{y}^2}{4\bar{x}}\right) \tag{4}$$

$$\frac{h}{h} - 1 = \frac{B}{\bar{x}^{1/2}} \exp\left(-\frac{\sigma \bar{y}^2}{4\bar{x}}\right) \tag{5}$$

where A and B are determined from the initial conditions

$$A = \frac{1}{2}\left(\frac{Re_d}{\pi}\right)^{1/2} \left(\frac{\rho_e u_e \theta}{\rho_\infty u_\infty d} M^2\right)_0 \tag{6}$$

$$B = \frac{(\sigma Re_d)^{1/2}}{2\pi^{1/2}(\rho_\infty u_\infty d) h_0} [Q + (\rho u^3 \theta)_0] \tag{7}$$

θ is the momentum thickness

$$\theta = 2 \int_0^\infty \frac{\rho u}{\rho_e u_e} \left(1 - \frac{u}{u}\right) dy \tag{8}$$

Q is the heat transfer to the body, and σ is the Prandtl number

From Eq 6,

$$\frac{\theta}{\theta_0} = \frac{(\rho_e u M_e^2)_0}{\rho u_e M^2} \tag{9}$$

As shown in the given equations, the value of the momentum thickness and wake width at the neck must be known as initial conditions for theoretical analyses Lees and Hi omas have estimated these quantities and have shown that they should vary as $(Re_d)^{-1/2}$ based on estimates of skin friction around the body and the pressure rise at the neck Experimental values, based on the present tests, are shown in Fig 9 Here 11 points are plotted corresponding to the combinations of cylinder diameter and Reynolds number given in Table 1 The wake width was obtained from pitot-pressure measurements, and the momentum thickness was calculated from experimental data The axial location of the neck was taken at $x/d = 2.50$ for the 0.300-in.-diam cylinder and $x/d = 3.00$ for the other models Figure 9 shows that these quantities do vary as $(Re_d)^{-1/2}$ The data scatter is probably due to the effect of the velocity gradient on pitot measurements [18]

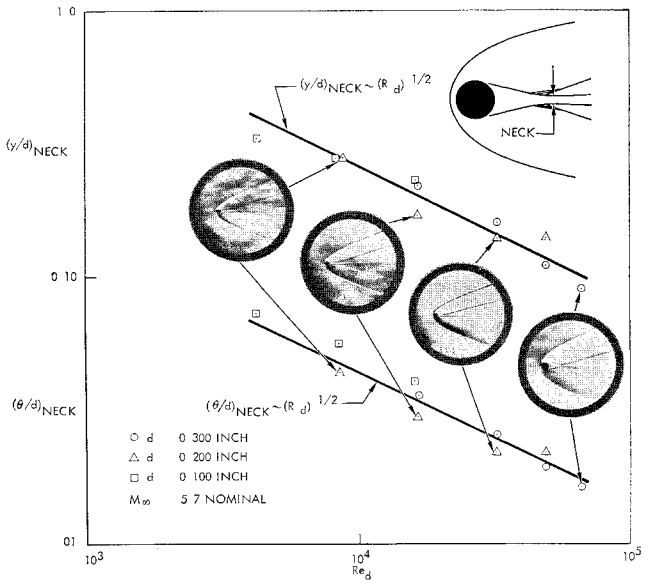

Fig 9 Wake width and momentum thickness at neck

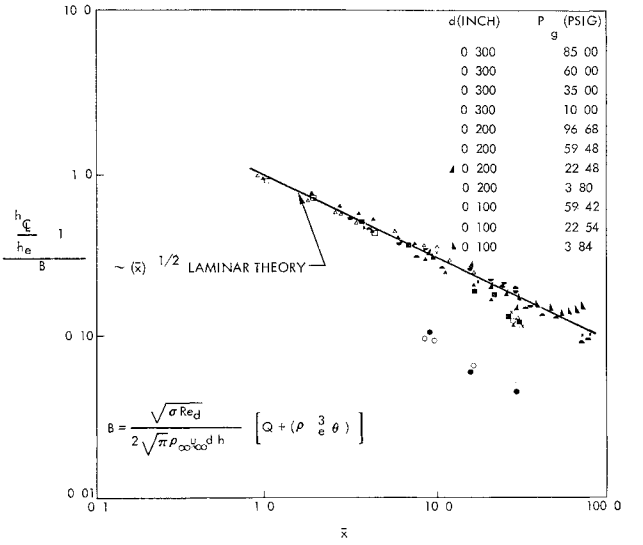

Fig 10 Static-enthalpy excess along wake centerline

The analysis shows that the static-enthalpy excess $(h/h) - 1$ and the velocity defect $M_e^2 w$ vary as $(\bar{x})^{-1/2}$ along the wake centerline The results from the experiments are plotted in Figs 10 and 11 These figures show that there is a Reynolds number similitude as indicated by the laminar theory The two runs that do not correspond with the base line are interpreted to be fully turbulent It should be noted that the static-enthalpy excess and the velocity defect for the turbulent case also vary as $(\bar{x})^{-1/2}$, when turbulence is fully established The representations of Figs 10 and 11 can also be used as measures of transition At transition, the values of static-enthalpy excess and velocity defect decrease much more rapidly than for the laminar case because of more efficient mixing processes

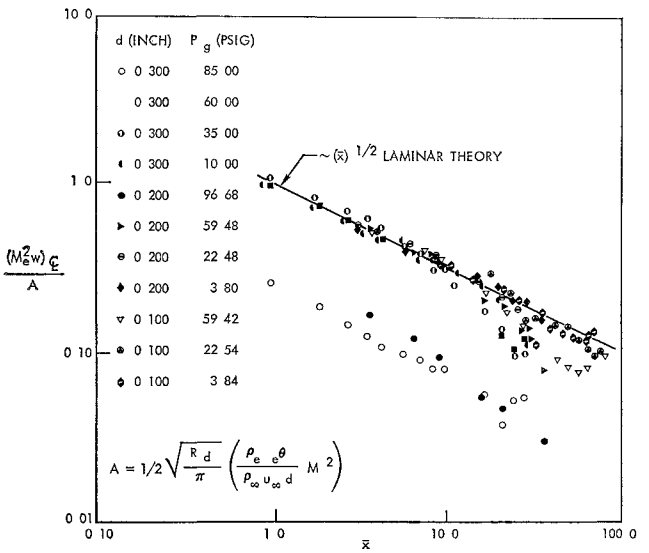

Fig 11 Velocity defect along wake centerline

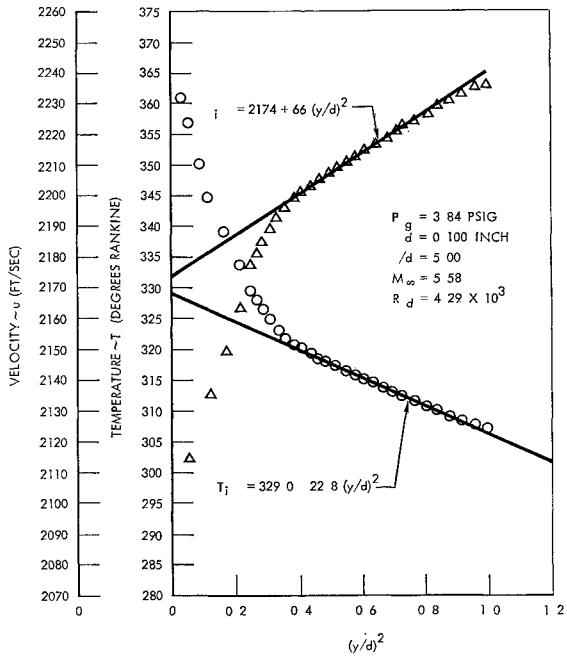

Fig 12 Determination of inviscid values of velocity and temperature

Since the velocity and the temperature in the inviscid flow outside of the viscous wake vary parabolically with vertical distance, the viscous contribution to the profile was obtained by subtracting the extrapolation of the inviscid profile into the viscous region When the velocity and the temperature from the experiment are plotted against the square of the distance from the wake centerline as in Fig 12, the points lying outside the viscous wake fall on a straight line, which can be easily extended into the viscous region The viscous profiles thus obtained are plotted in Figs 13 and 14 for the lower Reynolds number cases in Table 1 The form of the abscissa is suggested by the foregoing analysis and avoids the ambiguity of defining the wake edge The additive constant $\bar{x}_0$ in Figs 13 and 14 is the location of the virtual origin of the wake, determined from the variation of the centerline velocity and temperature [18] For the 0 100-in model, there is good agreement between the experiment and the linearized theory beyond nine diameters downstream Evidently, for the region of the wake closer to the neck, the constant convection assumption used for linearization ($w \ll 1$) is no longer valid

Lees and Hromas assumed the Townsend value of "universal" turbulent Reynolds number of 12 5 for the centerline conditions in the turbulent wake To investigate this assumption experimentally, consider the momentum equation at the centerline:

$$\rho_{\text{℄}}\, u_{\text{℄}} \left(\frac{\partial u}{\partial x}\right)_{\text{℄}} + \frac{dp}{dx} = \rho_{\text{℄}} (\epsilon_T)_{\text{℄}} \left(\frac{\partial^2 u}{\partial y^2}\right)_{\text{℄}} \tag{10}$$

In order to obtain $\partial^2 u/\partial y^2$ without differentiating experimental data twice, the method first proposed by Kingsland to reduce diffusion measurements was used Assuming that the velocity profile near the center is close to Gaussian,

$$\frac{w}{w_{\text{℄}}} \doteq \exp\left[-\frac{1}{D_N}\left(\frac{y}{d}\right)^2\right] \tag{11}$$

Then it follows that

$$\left[\frac{\partial^2 u}{\partial (y/d)^2}\right]_{\text{℄}} = u\, \frac{2 w_{\text{℄}}}{D_N} \tag{12}$$

and

$$D_N = \lim_{y\to 0} \frac{(y/d)^2}{\ln(w_{\text{℄}}/w)} = \lim_{y\to 0}\left[\frac{(y/d)}{\ln (w_{\text{℄}}/w)^{1/2}}\right]^2 \tag{13}$$

By plotting the parameter $\ln(w_{\text{℄}}/w)^{1/2}$ vs vertical distance near the centerline, Fig 15, it was possible to obtain the diffusivity number D_N

Once D_N is determined, $(\epsilon_T)_{\text{℄}}$ is given by

$$\tilde{\mu}_{\text{℄}} \equiv \left(\frac{\epsilon_T}{\nu}\right)_{\text{℄}} = \frac{D_N d^2 [\rho u (\partial u/\partial x) + (dp/dx)]_{\text{℄}}}{2\mu_{\text{℄}} (u_e - u_{\text{℄}})} \tag{14}$$

The expression on the right side of the foregoing relation is equal to unity in laminar wakes and greater than unity in turbulent wakes Figure 16 presents evaluations of this expression at several test conditions It shows that $\tilde{\mu}_{\text{℄}}$ is about unity for all stations in the wake in low Reynolds number cases, grows greater than unity at downstream stations in medium Reynolds number cases, and is larger than unity again throughout the wake in the highest Reynolds number case

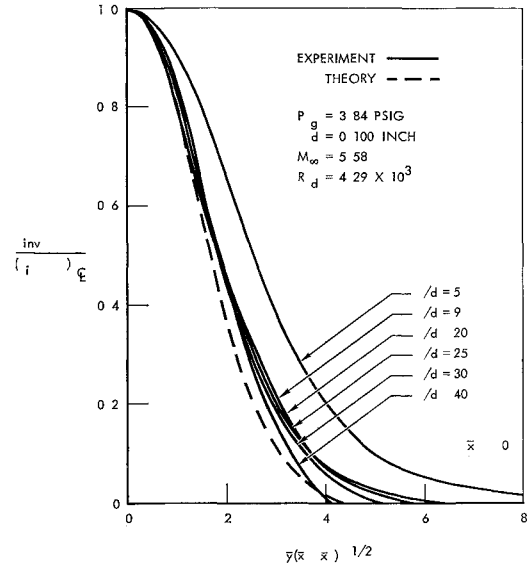

Fig 13a Normalized velocity profiles, 0 100-in -diam cylinder

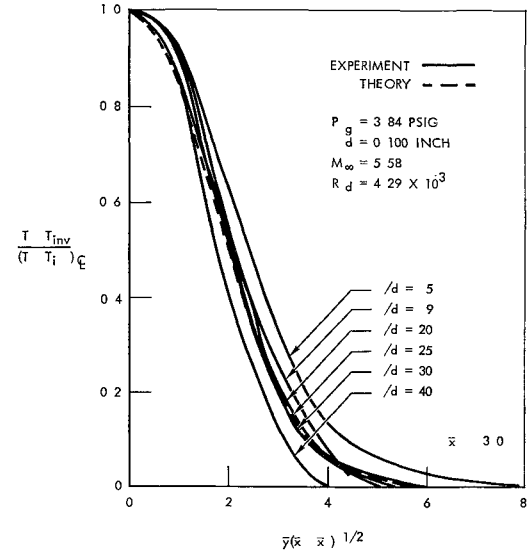

Fig 13b Normalized temperature profiles, 0 100-in -diam cylinder

A modified Townsend Reynolds number, Re_T, is defined by

$$Re_T = \frac{(u_e - u_{\mathfrak{C}})y_e}{\epsilon_T} \tag{15}$$

This definition of Re_T differs slightly from that of Ref 4, where, in place of y, the length used is the distance from the center at which the velocity defect is $e^{-1/2}$ of the maximum defect

To obtain experimental values of Re_T, it is necessary to differentiate two experimental quantities that subtract from each other to evaluate the turbulent diffusivity Therefore, the accurate determination of this quantity is very difficult In any case, the tentative value $Re_T = 10 \pm 5$ was obtained This value agrees with that used by Lees and Hromas in their theoretical treatment ($Re_T = 12.5$) The results also compare favorably with those of Kingsland, where he estimated the value $Re_T = 12$

Experimental Determination of Transition

As indicated in the foregoing discussion, a qualitative definition of transition could be obtained from plots of state properties along the centerline Another definition is possible by calculating the Townsend Reynolds number discussed previously

Using all available inputs, the results for these tests are superimposed on those of Demetriades[13] in Fig 17 For the 11 runs shown in Table 1, seven transition points could be obtained, two cases being fully laminar and two cases fully turbulent The comparison with Demetriades' data is surprisingly good Since the edge properties could be determined with the present measurements, it was possible to define a transition Reynolds number based on local conditions and distance from an effective origin Its value was calculated as 85,000

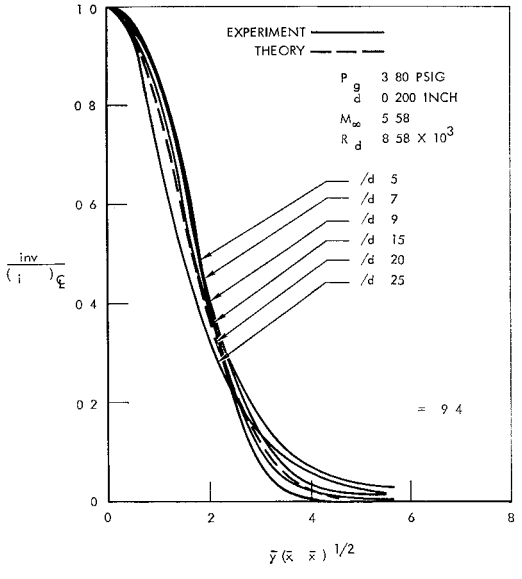

Fig 14a Normalized velocity profiles, 0 200-in -diam cylinder

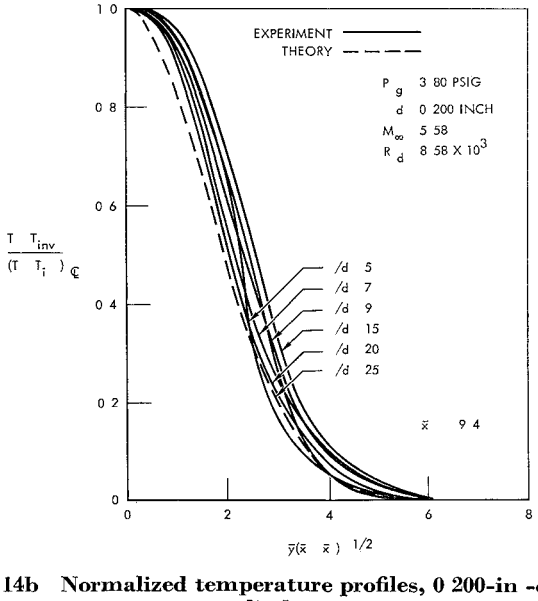

Fig 14b Normalized temperature profiles, 0 200-in -diam cylinder

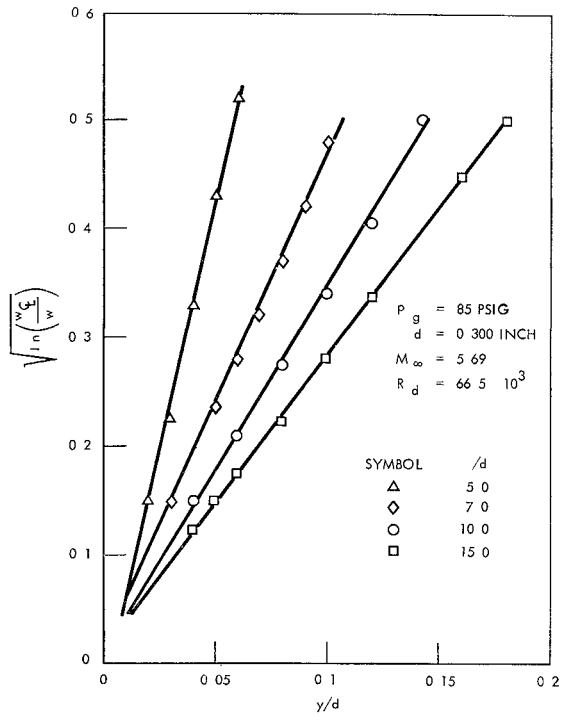

Fig 15 Determination of diffusivity number

Conclusions

An experimental investigation has been made of the flow behind a circular cylinder at a nominal freestream Mach number of 5 7 The Reynolds number was varied by chang-

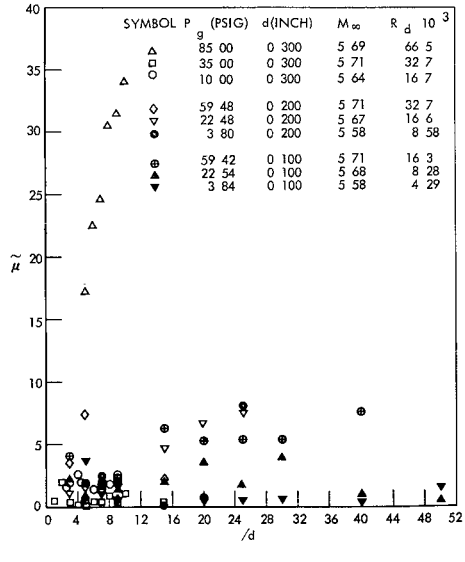

Fig 16 Viscosity parameter vs axial distance

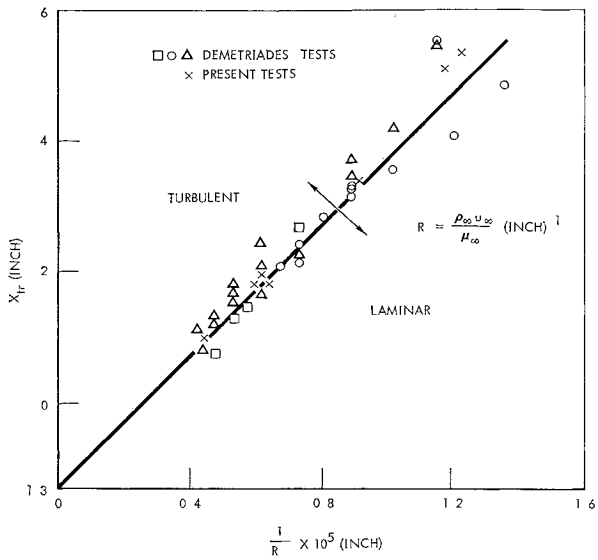

Fig 17 Transition

ing both the diameter of the cylinder and the stagnation pressure of the wind tunnel (the former over a three-fold range and the latter over an eight-fold range) Sufficient measurements were made to define completely the flow field at various stations downstream

From these measurements, it is concluded that 1) the base-flow region is laminar for the entire range of Reynolds number in the present experiment, 2) static pressure is nearly constant across the wake, 3) the near wake is laminar for low Reynolds number cases and becomes turbulent as Reynolds number is increased, and 4) the transition in the wake occurs when the Reynolds number based on edge conditions and the distance from the body exceeds 85,000 §

Correlation of the experimental data with a linearized theory for laminar flow was made The theoretical prediction of centerline values of static enthalpy and local velocity based on this theory were in good agreement with the experimental results Distributions of static enthalpy and local velocity in the wake agree with the theory for downstream stations greater than about nine diameters, if provision is made for an "effective" origin based on the axial distribution of the velocity and the enthalpy at the centerline

A qualitative experimental value of the Townsend Reynolds number for turbulent flow on which the theory of Lees and Hromas is based was obtained Its value was determined as $Re_T = 10 \pm 5$ In the present experiments, accurate definition of the turbulent wake was very difficult since the pitot-pressure defect decays very rapidly in the turbulent wake Further experiments are needed to investigate the turbulent wakes in hypersonic flow, especially the effect of interaction with external vorticity

References

[1] Goldstein, S (ed), *Modern Developments in Fluid Dynamics* (Oxford University Press, London, 1938) Vol II, Chap XIII

[2] Schlichting, H , *Boundary Layer Theory* (McGraw-Hill Book Co , Inc , New York, 1960), 4th ed , Chaps IX and XXIII

[3] Birkhoff, G and Zarantonello, E H , *Jets, Wakes, and Cavities* (Academic Press Inc , New York, 1957), Chaps XII–XIV

[4] Townsend, A A , *The Structure of Turbulent Shear Flow* (Cambridge University Press, London, 1956), Chap 7

[5] Roshko, A , "On the drag and shedding frequency of bluff cylinders," NACA TN 3169 (July 1954)

[6] Cooper, R D and Lutzky, M , "Exploratory investigation of the turbulent wakes behind bluff bodies," The David W Taylor Model Basin, Research and Development Rept 963 (October 1955)

[7] Feldman, S , "On trails of axi-symmetric hypersonic blunt bodies flying through the atmosphere," Avco-Everett Research Lab , Research Rept 82 (December 1959); also, J Aerospace Sci **28,** 433–448, 470 (June 1961)

[8] Lykoudis, P S , "Theory of iodized trails for bodies at hypersonic speeds," The Rand Corp Rept RM-2682-1-PR (October 5, 1961)

[9] Lees, L and Hromas, L , "Turbulent diffusion in the wake of a blunt-nosed body at hypersonic speeds," Space Technology Labs , Inc , Aerodynamics Dept Rept 50 (July 1961); also IAS Paper 62-71 (January 1962)

[10] Kubota, T , "Laminar wake with steamwise pressure gradient," Graduate Aeronautical Lab , California Institute of Technology, Hypersonic Research Project, Internal Memo 9 (May 1, 1962)

[11] Slattery, R E and Clay, W G , "Width of the turbulent trail behind a hypervelocity sphere," Massachusetts Institute of Technology, Lincoln Lab Rept 35G-0004 (June 6, 1961)

[12] Dana, T A and Short, W W , "Experimental study of hypersonic turbulent wakes," Convair, San Diego, Calif , Rept ZPh-103 (May 29, 1961)

[13] Demetriades, A , "Some hot-wire anemometer measurements in a hypersonic wake," *Proceedings of the 1961 Heat Transfer and Fluid Mechanics Institute* (Stanford University Press, Stanford, Calif , 1961)

[14] Mohlenhoff, W , 'Experimental study of helium diffusion in the wake of a circular cylinder at M = 5 8," Graduate Aeronautical Lab , California Institute of Technology, Hypersonic Research Project Memo 54 (May 20, 1960)

[15] Kingsland, L , Jr , 'Experimental study of helium and argon diffusion in the wake of a circular cylinder at M = 5 8," Graduate Aeronautical Lab , California Institute of Technology, Hypersonic Research Project Memo 60 (June 1, 1961)

[16] Dewey, C F , Jr , "Hot wire measurements in low Reynolds number hypersonic flows," Graduate Aeronautical Lab , California Institute of Technology, Hypersonic Research Project Memo 63 (September 15, 1961); also ARS J **31,** 1709–1718 (1961)

[17] 'Semi-annual status report," Graduate Aeronautical Lab , California Institute of Technology, Hypersonic Research Project (April 1962)

[18] McCarthy, J F , Jr , "Hypersonic wakes," Ph D Thesis, Aeronautics Dept , California Institute of Technology (1962); also Graduate Aeronautical Lab , California Institute of Technology, Hypersonic Research Project Memo 67 (July 2, 1962)

[19] McCarthy, J F , Jr and Kubota, T , "A study of wakes behind a circular cylinder at M = 5 7," AIAA Paper 63-170 (June 1963)

[20] Baloga, P E and Nagamatsu, H T , Instrumentation of GALCIT hypersonic wind tunnels," Graduate Aeronautical Lab , California Institute of Technology, Memo 29 (July 31, 1955)

[21] Tewfik, O K and Giedt, W H , "Heat transfer, recovery factor and pressure distributions around a cylinder normal to a supersonic rarefied air stream: Part I, Experimental data," Univ California, Berkeley TR HE-150-162 (January 30, 1959); also J Aerospace Sci **27,** 721–729 (October 1960)

[22] Mathews, M L , "An experimental investigation of viscous effects on static and impact pressure probes in hypersonic flow," Graduate Aeronautical Lab , California Institute of Technology, Hypersonic Research Project Memo 44 (June 2, 1958)

[23] Hayes, W D and Probstein, R F , *Hypersonic Flow Theory* (Academic Press Inc , New York, 1959), p 349

[24] Demetriades, A and Gold, H , "Transition to turbulence in the hypersonic wake of blunt-bluff bodies," ARS J **32,** 1420–1421 (September 1962)

§ Further discussion of transition incorporating these data is given in Ref 24